Paper IV

The 8.2 ka event: abrupt transition of the subpolar gyre toward a modern North Atlantic circulation[1]

Born, A. and A. Levermann (2010)

Click Here for Full Article

The 8.2 ka event: Abrupt transition of the subpolar gyre toward a modern North Atlantic circulation

A. Born

Bjerknes Centre for Climate Research, Allégaten 55, N-5007 Bergen, Norway (andreas.born@bjerknes.uib.no)

Also at Geophysical Institute, University of Bergen, N-5007 Bergen, Norway

A. Levermann

Potsdam Institute for Climate Impact Research, D-14412 Potsdam, Germany

Also at Institute of Physics, Potsdam University, D-14469 Potsdam, Germany

[1] Climate model simulations of the 8.2 ka event show an abrupt strengthening of the Atlantic subpolar gyre that allows us to connect two major but apparently contradictory climate events of the early Holocene: the freshwater outburst from proglacial lakes and the onset of Labrador Sea water formation. The 8.2 ka event is the largest climatic signal of our present interglacial with a widespread cooling in the North Atlantic region about 8200 years before present. It coincides with a meltwater outburst from North American pro-glacial lakes that is believed to have weakened the Atlantic meridional overturning circulation and north-ward heat transport, followed by a recovery of the deep ocean circulation and rising temperatures after a few centuries. Marine proxy data, however, date the onset of deep water formation in Labrador Sea to the same time. The subsequent strengthening of the slope current system created a regional signal recorded as an abrupt and persistent surface temperature decrease. Although similarities in timing are compelling, a mechanism to reconcile these apparently contradictory events was missing. Our simulations show that an abrupt and persistent strengthening of the Atlantic subpolar gyre provides a plausible explanation. The intense freshwater pulse triggered a transition of the gyre circulation into a different mode of operation, stabilized by internal feedbacks and persistent after the cessation of the perturbation. As a direct consequence, deep water formation around its center intensifies. This corresponds to the modern flow regime and stabilizes the meridional overturning circulation, possibly contributing to the Holocene's climatic stability.

1. Introduction

[2] During the relatively stable conditions of our present interglacial, the 8.2 ka event is the largest climatic signal with a widespread cooling in the North Atlantic region about 8200 years before present. It coincides with a meltwater outburst from North American proglacial lakes [*Alley et al.*, 1997; *Alley and Áugústsdóttir*, 2005, and references therein]. In current understanding, this caused a weakening of the Atlantic meridional overturning circulation (AMOC) and a subsequent reduction in northward heat transport, followed by a recovery of the deep ocean circulation and rising temperatures after a few centuries [*Bauer et al.*, 2004; *Hall et al.*, 2004; *Ellison et al.*, 2006; *Wiersma et al.*, 2006; *Kleiven et al.*, 2008].

[3] This two-dimensional explanation, however, is not able to explain a number of marine paleo-records that clearly call for a three-dimensional mechanism. An abrupt but persistent surface temperature decrease was reported from the western North Atlantic at the time of the 8.2 ka event (Figure 1) [*Solignac et al.*, 2004; *de Vernal and Hillaire-Marcel*, 2006; *Sachs*, 2007]. It has been suggested to be associated with the onset of deep water formation in Labrador Sea and a subsequent strengthening of the slope current system, the western branch of the subpolar gyre (SPG) [*Hillaire-Marcel et al.*, 2001; *Sachs*, 2007]. Proxy data from Reykjanes Ridge shows a similarly abrupt and persistent warming which provides evidence for an enhanced Irminger Current (Figure 1) [*Andersen et al.*, 2004; *Came et al.*, 2007]. This is the northeastern branch of the SPG and thus corroborates the hypothesis of a stronger gyre and enhanced convection in its center.

[4] The concurrence of these two events raises the question of how convection can increase at the time of the most severe freshwater flood of the past 10,000 years. We argue, based on coupled climate model experiments, that this is no contradiction but that a causal relationship connects the two events. A change in the density structure is found to provide positive feedbacks leading to a permanent strengthening of the SPG and convection. The impact of baroclinic adjustments on the SPG strength is well documented [*Eden and Willebrand*, 2001; *Häkkinen and Rhines*, 2004; *Hátún et al.*, 2005; *Treguier et al.*, 2005; *Levermann and Born*, 2007; *Born et al.*, 2009; *Lohmann et al.*, 2009; *Born et al.*, 2010; *Montoya et al.*, 2010] and this study aims to apply this physical understanding to data from the geological record.

2. Model Description

[5] To investigate the role of the SPG during the 8.2 ka event we make use of the coupled climate model CLIMBER-3α, which comprises atmosphere and sea ice components and the oceanic general circulation model MOM-3 (*Montoya et al.* [2005] and auxiliary material).[1] The oceanic horizontal resolution is 3.75° × 3.75° with 24 unevenly spaced vertical layers. Simplified atmosphere dynamics are solved on a coarse numerical grid (7.5° in latitude and 22.5° in longitude).

[6] Due to the coarse resolution of the model, the SPG and deep water formation in its center are shifted eastward and simulated boundary currents are relatively broad (Figure 2). A second deep water formation region is found in the Nordic seas. Despite shortcomings, the interaction between gyre advection, convection in its center and eddy transport in between, as well as the communication of deep water masses across the deepest passages of the Greenland-Scotland ridge, compares well to higher-resolution models [*Spall*, 2005; A. Born et al., Late Eemian warming in the Nordic seas as seen in proxy data and climate models, submitted to *Paleoceanography*, 2010]. For additional information we refer to sensitivity studies with glacial [*Montoya et al.*, 2010] and present-day boundary conditions [*Mignot et al.*, 2006] as well as under global warming [*Levermann et al.*, 2007].

[7] For the present study, the model was initialized with climatological hydrography [*Levitus*, 1982] and orbital parameters for 8,200 years before present [*Berger*, 1978]. Atmospheric CO_2 concentration was set to 260 ppm [*Raynaud et al.*, 2000]. The continental watershed over North America was shifted to the west and south in order to take into account changes in surface gradient due to the isostatic depression of glacial ice sheets. After the model was run into equilibrium over 2700 years, the simulated SPG exhibits a stable but weak volume transport of 19.5 Sv (1 Sv = 10^6 m^3 s^{-1}). In order to simulate the lake drainage, 160 · 10^{12} m^3 of freshwater were added to the surface of the Labrador Sea coast during a period of two years, west of the deep convection region. This value is equivalent to a 2 year volume

---

[1]Auxiliary materials are available in the HTML. doi:10.1029/2009GC003024.
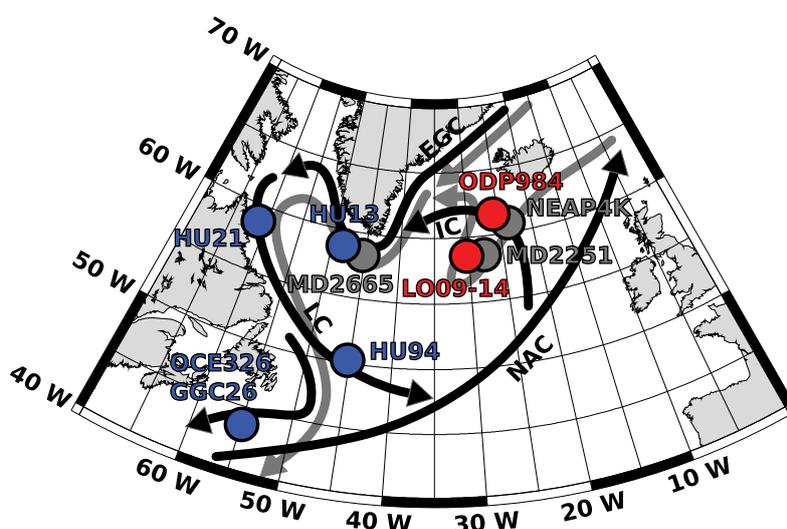
Figure 1. Map of the subpolar North Atlantic showing the location of core sites and of major ocean currents mentioned in the text. Blue dots denote cores that show an abrupt and persistent cooling after 8 ka before present; warming is reported from the Reykjanes Ridge and marked red. Grey dots show where the 8.2 ka event is evident as a temporal reduction in deep current flow speed. Black arrows illustrate the surface currents (IC, Irminger Current; EGC, East Greenland Current; LC, Labrador Current; NAC, North Atlantic Current); grey arrows illustrate the Deep Western Boundary Current. For a list of full core names and references, please refer to Table S1 in Text S1.

flux of 2.6 Sv, based on a recent estimate of the lake volume [*Leverington et al.*, 2002], and has been used in previous model studies [*Bauer et al.*, 2004; *LeGrande et al.*, 2006; *Wiersma et al.*, 2006]. For diagnostic purposes, a passive tracer was released simultaneously with the freshwater flux at the same location in order to track advection of the perturbation. This tracer does not influence the circulation. We define the strength of the subpolar gyre as the local minimum of the depth integrated stream function. For the cyclonic circulation of the SPG, this stream function is negative (Figure 2).

3. Model Results and Interpretation of Proxy Data

[8] In response to the meltwater release, the SPG switches into a significantly stronger mode with 29 Sv volume transport (Figures 2 and 3a). This represents a strengthening of about 50% and the stronger circulation is within the uncertainty of present-day observations [*Bacon*, 1997; *Read*, 2001]. Further integration shows that this stronger state is stable and not only a temporary response to the freshwater pulse.

[9] The abrupt transition is due to two positive feedbacks inherent to the SPG [*Levermann and Born*, 2007]. First, a stronger SPG transports less tropical saline water into the Nordic seas but accu-

mulates these in the subpolar North Atlantic, making upper water masses in the center of the SPG more saline (Figures S7–S9 in Text S1). This is consistent with previous conclusions which are based on simulations with a high-resolution ocean general circulation model and confirmed by observations [*Hátún et al.*, 2005; *Lohmann et al.*, 2009]. Increased surface salinity enhances deep convection, cooling the deep water column. Besides, a stronger SPG results in enhanced outcropping of isopycnals
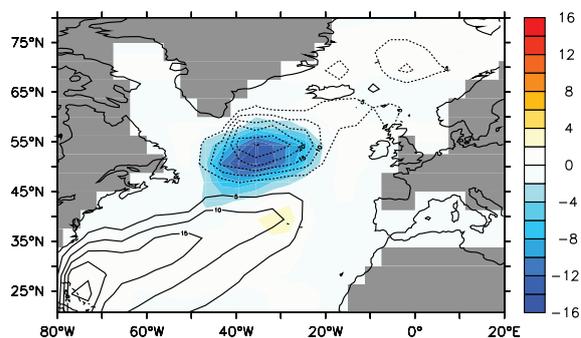

Figure 2. Colors indicate anomaly of the vertically integrated stream function, last 50 years of the perturbed simulation minus last 50 years before the meltwater pulse. Contours indicate vertically integrated stream function for the last 50 years of the simulation. For the cyclonic circulation of the SPG, the negative anomaly represents a strengthening. Outside the subpolar North Atlantic, currents are virtually unchanged.
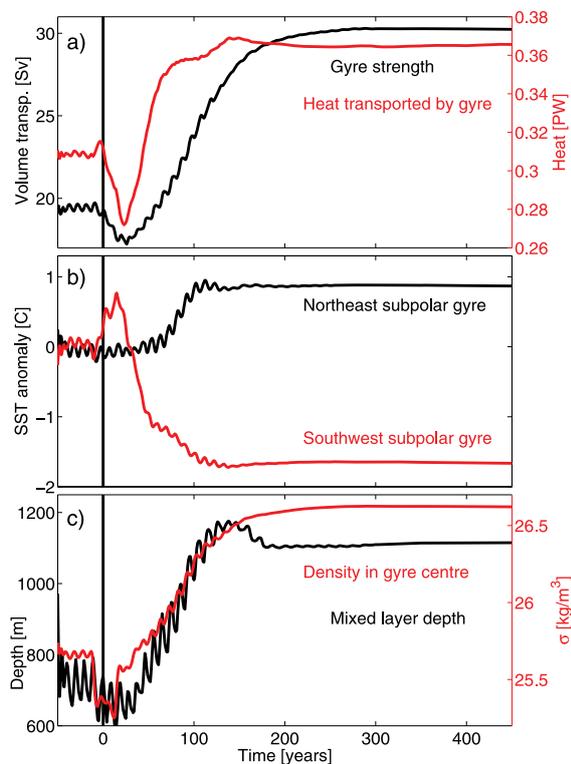
Figure 3. Temporal evolution of key quantities of the transition toward a stronger SPG during the 8.2 ka event. The vertical line indicates the timing of the lake Agassiz drainage; data are filtered with a 25 year running mean. (a) Volume and heat transport of the SPG, (b) sea surface temperature in the northeastern (black) and southwestern (red) subpolar region, and (c) maximum winter mixed layer depth in the center of the SPG and surface density in the center of the SPG (see Figure S7 in Text S1). The stronger heat transport leads to a warming of the northeastern gyre region while the southwestern part cools rapidly. Surface density and mixed layer depth increase simultaneously.

and hence a more efficient removal of heat from the gyre's center by isopycnal mixing. Both effects, salt accumulation and removal of heat, increase the core density of the gyre compared to the relatively light exterior, sea surface drops and the corresponding geostrophic response strengthens the cyclonic SPG circulation.

[10] In addition to these self-sustaining internal feedbacks, there exists an interaction with the flow over the Greenland-Scotland ridge. The meltwater perturbation reduces sinking in the Nordic seas and therewith the supply of dense overflow waters to the northern rim of the SPG. Consequently, the outer rim of the gyre gets lighter and the gyre slightly intensifies. This triggers the two internal feedbacks mentioned above and yields the stronger SPG state

(Figure S1 in Text S1). Elsewhere, we have shown that a short reduction of dense deep outflow from the Nordic seas is sufficient to trigger the transition (≥25 years [*Levermann and Born*, 2007]) and that the described internal feedbacks dominate the dynamics. Changes in wind stress are small and do not show a consistent pattern (Figure S6 in Text S1). This is plausible because the freshwater flood does not impact wind patterns directly. Moreover, the coarse resolution of the atmosphere component might underestimate regional variations. Thus, the changes in wind stress seen after the transition are likely due to local changes in sea ice as suggested also by the irregular pattern. The mechanism of transition is robust to prescribed wind forcing and with respect to model setup and experimental design (see auxiliary material).

[11] Considering this change in surface circulation allows us to combine a number of proxy records into a consistent picture of the 8.2 ka event. Recent work found strong evidence for a reduction of dense water supply from the Nordic seas due to the lake Agassiz drainage [*Hall et al.*, 2004; *Ellison et al.*, 2006; *Kleiven et al.*, 2008]. However, proxy data suggests that the meltwater signal did not reach the convection region at the center of the Labrador Sea but was exported along the shelf in the Labrador Current [*Keigwin et al.*, 2005; *Hillaire-Marcel et al.*, 2007]. From there a large portion moved northeastward and was diluted by mixing with water of the North Atlantic Current before reaching the Nordic seas and causing a moderate reduction in convection there. Our model reproduces this path qualitatively. 30 years after the lake drainage, highest concentrations of meltwater are found in the Nordic seas where 25% of the meltwater pulse has been advected to (Figure 4).

[12] After the transition, the stronger SPG circulation intensifies oceanic heat transport (Figure 3a). More warm tropical water reaches the northern SPG while more cold water is advected toward the west and south. This results in a sea surface temperature (SST) dipole (Figure S7 in Text S1). The southwestern SPG region cools abruptly (Figure 3b, red) while rapid warming is seen in the northeastern SPG region (Figure 3b, black).

[13] An abrupt and persistent SST decrease coeval with the lake drainage has indeed been reported from dinoflagellate cysts and alkenones for many locations throughout Labrador Sea and downstream Labrador Current south of Newfoundland [*Solignac et al.*, 2004; *de Vernal and Hillaire-Marcel*, 2006; *Sachs*, 2007]. Consistent with our simulations this
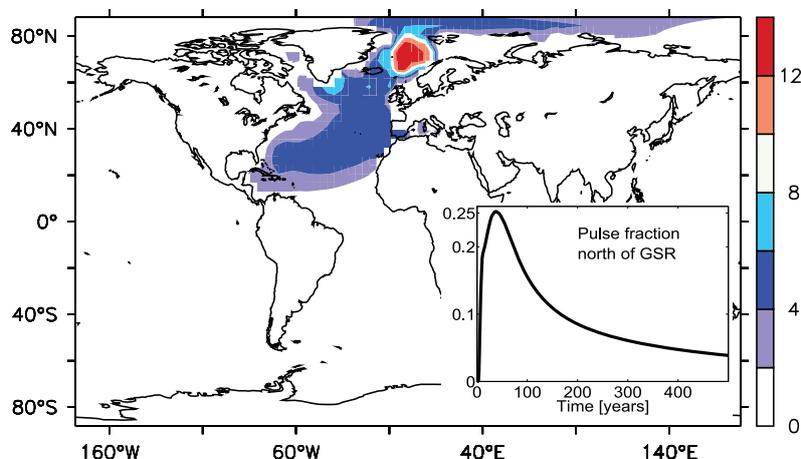
Figure 4. Distribution of the meltwater pulse 30 years after its release into the Labrador Sea, integrated over depth (in m). Highest concentrations are found in the Nordic seas. Inset shows the fraction of the pulse in the Nordic seas and the Arctic Ocean. After approximately 30 years, 25% of the meltwater is advected north of the Greenland-Scotland ridge, followed by a decline as it is diluted globally.

data indicates a drastic reorganization of the slope current system. No persistent cooling is seen in foraminiferal data from Eirik Drift in the northern Labrador Sea, probably because of its location too far offshore to record changes in the coastal current [*Kleiven et al.*, 2008]. The warming signal on the eastern side of the gyre is not easily detected in proxy records because the strengthening of the surface circulation also changed the position of frontal systems. Thus, the strengthening of the SPG is recorded as a subsurface cooling inferred from foraminifera at a relatively eastern location [*Thornalley et al.*, 2009]. However, approximately 400 km further west on Reykjanes Ridge, where currents are more constrained by topography, an increase and stabilization of surface temperatures reconstructed using diatoms, foraminiferal $\delta^{18}O$ and Mg/Ca data has been associated with an intensification of the Irminger Current, the northern limb of the SPG (Figure 1) [*Andersen et al.*, 2004; *Came et al.*, 2007].

[14] Further support for a transition toward a stronger SPG following the 8.2 ka event comes from increased sea surface salinities throughout the subpolar region that started similarly abrupt as the temperature changes and were equally persistent, both in our model experiments (Figures S7–S9 in Text S1) and proxy data [*Solignac et al.*, 2004; *de Vernal and Hillaire-Marcel*, 2006; *Hillaire-Marcel et al.*, 2007; *Came et al.*, 2007]. The cooling of western slope waters can thus not be attributed to more intense transport of cold and fresh Arctic waters through the East Greenland Current. Their upstream source must be the rela-

tively saline Irminger Current which suggests a SPG intensification. A sudden increase in advection of Atlantic water into Labrador Sea has also been concluded from diatoms, fossil shell data and foraminiferal assemblages at several locations along the Greenland west coast [*Donner and Jungner*, 1975; *Lloyd et al.*, 2005; *Ren et al.*, 2009]. The intensification of westward salt transport and the eastward movement of the subpolar front with a stronger SPG results in a freshening of inflow into the Nordic seas (Figure S7 in Text S1), consistent with paleo-observations [*Thornalley et al.*, 2009] and present-day instrumental records [*Hátún et al.*, 2005]. Salt accumulation in the center of a anomalously strong SPG has been shown in a higher-resolution model [*Lohmann et al.*, 2009].

[15] Proxy data of Labrador Sea convection furthermore supports a significant reorganization of the surface circulation. In our simulations, enhanced surface salinity together with subsurface cooling in the center of the SPG results in a density increase and a subsequent intensification of convection south of the Greenland-Scotland ridge (Figure 3c). These results match well with existing data of the geological record. Little or no Labrador Sea Water was produced in the early Holocene and formation intensified not long after the meltwater outburst [*Hillaire-Marcel et al.*, 2001, 2007]. Isotopic changes in Labrador Sea sediments show a persistent reorganization of the deep current system after 8,000 years before present [*Fagel et al.*, 2004] with deeper Labrador Sea Water found in Pa/Th data [*Gherardi et al.*, 2009] and a permanent reduction of deep water formed in the Nordic seas
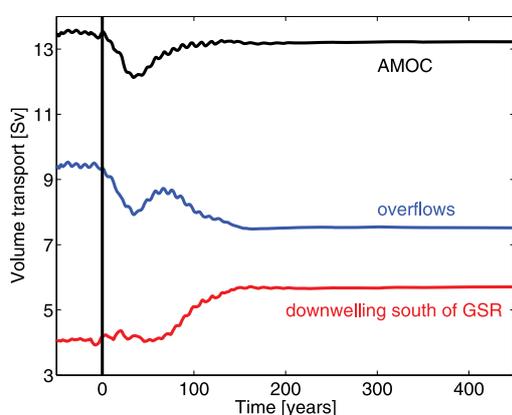
Figure 5. The Atlantic Meridional Overturning Circulation (AMOC), decomposed into deep water contributions from sinking in the Nordic seas (blue) and south of the Greenland-Scotland ridge (red). The vertical line indicates the timing of the lake Agassiz drainage, and a 25 year running mean filter is applied. The AMOC weakens abruptly in response to the freshwater event and recovers gradually over approximately 100 years. While the initial weakening is caused by the reduction of deep water supply from the Nordic seas, the recovery is due to a delayed intensification of Labrador Sea deep water formation. Both Nordic seas and Labrador Sea downwelling change significantly and persistently.

recorded in benthic $\delta^{13}C$ data [*Evans et al.*, 2007]. This points toward a persistent reorganization of both the horizontal surface and the deep meridional circulation, as simulated here.

[16] In contrast to significant changes in SPG strength (47%), the AMOC weakens by just 1.5 Sv (11%) in response to the meltwater pulse, significantly less than the 30%–50% reduction reported from previous model studies [*Bauer et al.*, 2004; *Wiersma et al.*, 2006; *LeGrande et al.*, 2006] (Figure 5). The strong response in earlier simulations might be due to the application of the meltwater pulse directly on the Labrador Sea convection region with dramatic consequences for SPG and AMOC. Such a freshwater perturbation leads to a reduction of convection in the Labrador Sea contradicting the paleorecord that shows the intensification of convection in this region. Moreover, this scenario removes a significant fraction of the freshwater pulse from the surface, inconsistent with proxy data indicating its advection in the Labrador Current. Hence, a smaller fraction is advected into the Nordic seas which is crucial to initiate the mechanism amplifying the SPG as discussed above (see auxiliary material for further discussion). The initial AMOC weakening in our simulation is followed by a rapid recovery over approximately 100 years and then a more gradual

increase. The decomposition into deep water formation regions shows that the initial weakening is due to reduced sinking in the Nordic seas, reaching its minimum after 150 years. The recovery and weak overall reduction is due to an increase in deep water formation south of the Greenland-Scotland ridge with a time lag of approximately 50 years (Figures 5 and 3c).

[17] A distinctive reduction in deep current flow speeds, probably delayed by at least several decades, is reported from the Greenland-Scotland ridge overflows and off the southern tip of Greenland (Figure 1) [*Hall et al.*, 2004; *Ellison et al.*, 2006; *Kleiven et al.*, 2008]. This is upstream from where Labrador Sea Water joins the Deep Western Boundary Current, the southward flowing branch of the AMOC. Further south in the North Atlantic, the reduction of northern source deep waters is minor for the 8.2 ka event if recorded at all [*Keigwin and Boyle*, 2000; *Oppo et al.*, 2003; *Keigwin et al.*, 2005]. The onset of Labrador Sea Water formation following the meltwater pulse might explain this discrepancy.

4. Summary and Conclusions

[18] Expanding previous studies that focused on the AMOC response, i.e., changes in the meridional circulation, to the lake Agassiz drainage, we propose that many observed but hitherto unexplained abrupt changes and discrepancies require taking into account a reorganization of the horizontal circulation. The most striking result is the persistent strengthening of the SPG in response to the short freshwater pulse. The transition between the two circulation patterns is triggered by an external positive feedback and stabilized by two positive feedback mechanisms within the SPG.

[19] While our results do not contradict an abrupt and considerable AMOC reduction in response to the lake Agassiz drainage, it might have been relatively short lived and weaker than suggested by previous simulations for two reasons: (1) The freshwater flood had the biggest impact not in the Labrador Sea but primarily affected deep water formation in the Nordic seas after mixing in the North Atlantic Current (Figure 4) and (2) this deep water reduction was partly compensated by enhanced sinking in the Labrador Sea (Figures 3c and 5). The latter mechanism has already been observed in models and data on time scales of several millennia [*Renssen et al.*, 2005; *Solignac et al.*, 2004].

[20] In our model the reorganization of the SPG surface circulation and subsequent changes in heat and salt advection provide the precondition for a more intense Labrador Sea convection and stabilize it. It has been suggested that this circulation mode is a unique feature of the Holocene, with Labrador Sea Water probably missing in the warmer climate of the last interglacial [*Hillaire-Marcel et al.*, 2001] and implications for the stability of the AMOC by the end of this century. Our results might provide the base for a future investigations of these hypotheses.

Acknowledgments

References

Alley, R. B., and A. M. Áugústsdóttir (2005), The 8k event: Cause and consequences of a major Holocene abrupt climate change, *Quat. Sci. Rev.*, *24*, 1123–1149.

Alley, R. B., P. A. Mayewski, T. Sowers, M. Stuiver, K. C. Taylor, and P. U. Clark (1997), Holocene climatic instability: A prominent, widespread event 8200 years ago, *Geology*, *25*, 483–486.

Andersen, C., N. Koc, and M. Moros (2004), A highly unstable Holocene climate in the subpolar North Atlantic: Evidence from diatoms, *Quat. Sci. Rev.*, *23*, 2155–2166.

Bacon, S. (1997), Circulation and fluxes in the North Atlantic between Greenland and Ireland, *J. Phys. Oceanogr.*, *27*, 1420–1435.

Bauer, E., A. Ganopolski, and M. Montoya (2004), Simulation of the cold climate event 8200 years ago by meltwater outburst from Lake Agassiz, *Paleoceanography*, *19*, PA3014, doi:10.1029/2004PA001030.

Berger, A. (1978), Long-term variations of caloric solar radiation resulting from the Earth's orbital elements, *Quat. Res.*, *9*, 139–167.

Born, A., A. Levermann, and J. Mignot (2009), Sensitivity of the Atlantic Ocean circulation to a hydraulic overflow parameterisation in a coarse resolution model: Response of the subpolar gyre, *Ocean Modell.*, *27*(3–4), 130–142.

Born, A., K. H. Nisancioglu, and P. Braconnot (2010), Sea ice induced changes in ocean circulation during the Eemian, *Clim. Dyn.*, doi:10.1007/s00382-009-0709-2, in press.

Came, R. E., D. W. Oppo, and J. F. McManus (2007), Amplitude and timing of temperature and salinity variability in the subpolar North Atlantic over the past 10 k.y., *Geology*, *35*, 315–318.

de Vernal, A., and C. Hillaire-Marcel (2006), Provincialism in trends and high frequency changes in the northwest North Atlantic during the Holocene, *Global Planet. Change*, *54*, 263–290.

Donner, J., and H. Jungner (1975), Radiocarbon dating of shells from marine deposits in the Disko Bugt, West Greenland, *Boreas*, *4*, 25–45.

Eden, C., and J. Willebrand (2001), Mechanism of interannual to decadal variability of the North Atlantic Circulation, *J. Clim.*, *14*, 2266–2280.

Ellison, C. R. W., M. R. Chapman, and I. R. Hall (2006), Surface and deep ocean interactions during the cold climate event 8200 years ago, *Science*, *312*, 1929–1932.

Evans, H. K., I. R. Hall, G. G. Bianchi, and D. W. Oppo (2007), Intermediate water links to Deep Western Boundary Current variability in the subtropical NW Atlantic during marine isotope stages 5 and 4, *Paleoceanography*, *22*, PA3209, doi:10.1029/2006PA001409.

Fagel, N., C. Hillaire-Marcel, M. Humblet, R. Brasseur, D. Weis, and R. Stevenson (2004), Nd and Pb isotope signatures of the clay-size fraction of Labrador Sea sediments during the Holocene: Implications for the inception of the modern deep circulation pattern, *Paleoceanography*, *19*, PA3002, doi:10.1029/2003PA000993.

Gherardi, J.-M., L. Labeyrie, S. Nave, R. Francois, J. F. McManus, and E. Cortijo (2009), Glacial-interglacial circulation changes inferred from ^{231}Pa/^{230}Th sedimentary record in the North Atlantic region, *Paleoceanography*, *24*, PA2204, doi:10.1029/2008PA001696.

Häkkinen, S., and P. B. Rhines (2004), Decline of subpolar North Atlantic circulation during the 1990s, *Science*, *304*, 555–559.

Hall, I. R., G. Bianchi, and J. R. Evans (2004), Centennial to millenial scale Holocene climate-deep water linkage in the North Atlantic, *Quat. Sci. Rev.*, *23*, 1529–1536.

Hátún, H., A. B. Sandø, H. Drange, B. Hansen, and H. Valdimarsson (2005), Influence of the Atlantic Subpolar Gyre on the thermohaline circulation, *Science*, *309*, 1841–1844.

Hillaire-Marcel, C., A. de Vernal, A. Bilodeau, and A. J. Weaver (2001), Absence of deep-water formation in the Labrador Sea during the last interglacial period, *Nature*, *410*, 1073–1077.

Hillaire-Marcel, C., A. de Vernal, and D. J. W. Piper (2007), Lake Agassiz Final drainage event in the northwest North Atlantic, *Geophys. Res. Lett.*, *34*, L15601, doi:10.1029/2007GL030396.

Keigwin, L. D., and E. A. Boyle (2000), Detecting Holocene changes in thermohaline circulation, *Proc. Natl. Acad. Sci. U. S. A.*, *97*, 1343–1346.

Keigwin, L. D., J. P. Sachs, Y. Rosenthal, and E. A. Boyle (2005), The 8200 year B.P. event in the slope water system, western subpolar North Atlantic, *Paleoceanography*, *20*, PA2003, doi:10.1029/2004PA001074.

Kleiven, H. F., C. Kissel, C. Laj, U. S. Ninnemann, T. O. Richter, and E. Cortijo (2008), Reduced North Atlantic Deep Water coeval with the glacial Lake Agassiz fresh water outburst, *Science*, *319*, 60–64.

LeGrande, A. N., G. A. Schmidt, D. T. Shindell, C. V. Field, R. L. Miller, D. M. Koch, G. Faluvegi, and G. Hoffmann (2006), Consistent simulations of multiple proxy responses to an abrupt climate change event, *Proc. Natl. Acad. Sci. U. S. A.*, *103*, 837–842.

Leverington, D., H. D. Mann, and J. T. Teller (2002), Changes in bathymetry and volume of glacial Lake Agassiz between 9200 and 7700 14C yr BP, *Quat. Res.*, *57*, 244–252.

Levermann, A., and A. Born (2007), Bistability of the Atlantic subpolar gyre in a coarse-resolution climate model, *Geophys. Res. Lett.*, *34*, L24605, doi:10.1029/2007GL031732.

Levermann, A., J. Mignot, S. Nawrath, and S. Rahmstorf (2007), The role of northern sea ice cover for the weakening of the thermohaline circulation under global warming, *J. Clim.*, *20*, 4160–4171.

Levitus, S. (1982), Climatological atlas of the world ocean, *NOAA Prof. Pap.*, *13*, 173 pp.

Lloyd, J., L. Park, A. Kuijpers, and M. Moros (2005), Early Holocene palaeoceanography and deglacial chronology of Disko Bugt, West Greenland, *Quat. Sci. Rev.*, *24*, 1741–1755.

Lohmann, K., H. Drange, and M. Bentsen (2009), Response of the North Atlantic subpolar gyre to persistent North Atlantic oscillation like forcing, *Clim. Dyn.*, *32*, 273–285.

Mignot, J., A. Levermann, and A. Griesel (2006), A decomposition of the Atlantic meridional overturning circulation into physical components using its sensitivity to vertical diffusivity, *J. Phys. Oceanogr.*, *36*, 636–650.

Montoya, M., A. Griesel, A. Levermann, J. Mignot, M. Hofmann, A. Ganopolski, and S. Rahmstorf (2005), The Earth system model of intermediate complexity CLIMBER-3α. Part I: Description and performance for present-day conditions, *Clim. Dyn.*, *25*, 237–263.

Montoya, M., A. Born, and A. Levermann (2010), Reversed North Atlantic gyre dynamics in present and glacial climates, *Clim. Dyn.*, doi:10.1007/s00382-009-0729-y, in press.

Oppo, D. W., J. F. McManus, and J. L. Cullen (2003), Deep-water variability in the Holocene epoch, *Nature*, *422*, 277–278.

Raynaud, D., J.-M. Barnola, J. Chappellaz, T. Blunier, A. Indermühle, and B. Stauffer (2000), The ice record of greenhouse gases: A view in the context of future changes, *Quat. Sci. Rev.*, *19*, 9–17.

Read, J. (2001), Water masses and circulation of the northeast Atlantic subpolar gyre, *Prog. Oceanogr.*, *48*, 461–510.

Ren, J., H. Jiang, M.-S. Seidenkrantz, and A. Kuijpers (2009), A diatom-based reconstruction of Early Holocene hydrographic and climatic change in a southwest Greenland fjord, *Mar. Micropaleontol.*, *70*, 166–176.

Renssen, H., H. Goosse, and T. Fichefet (2005), Contrasting trends in North Atlantic deep-water formation in the Labrador Sea and Nordic seas during the Holocene, *Geophys. Res. Lett.*, *32*, L08711, doi:10.1029/2005GL022462.

Sachs, J. P. (2007), Cooling of Northwest Atlantic slope waters during the Holocene, *Geophys. Res. Lett.*, *34*, L03609, doi:10.1029/2006GL028495.

Solignac, S., A. de Vernal, and C. Hillaire-Marcel (2004), Holocene sea-surface conditions in the North Atlantic—Contrasted trends and regimes in the western and eastern sectors (Labrador Sea vs. Iceland Basin), *Quat. Sci. Rev.*, *23*, 319–334.

Spall, M. A. (2005), Buoyancy-forced circulations in shallow marginal seas, *J. Mar. Res.*, *63*, 729–752.

Thornalley, D. J. R., H. Elderfield, and I. N. McCave (2009), Holocene oscillations in temperature and salinity of the surface North Atlantic, *Nature*, *457*, 711–714.

Treguier, A. M., S. Theetten, E. P. Chassignet, T. Penduff, R. Smith, L. Talley, J. O. Beismann, and C. Böning (2005), The North Atlantic Subpolar Gyre in four high-resolution models, *J. Phys. Oceanogr.*, *35*, 757–774.

Wiersma, A. P., H. Renssen, H. Goosse, and T. Fichefet (2006), Evaluation of different freshwater forcing scenarios for the 8.2 ka BP event in a coupled climate model, *Clim. Dyn.*, *27*, 831–849.

Supplementary Information for

The 8.2k event: abrupt transition of the subpolar gyre towards a modern North Atlantic circulation

Andreas Born[1]

Bjerknes Centre for Climate Research, Bergen, Norway

Geophysical Institute, University of Bergen, Bergen, Norway

Anders Levermann

Potsdam Institute for Climate Impact Research, Potsdam, Germany

Institute of Physics, Potsdam University, Potsdam, Germany

This Supplement is organized as follows: The climate model is described in detail in section 1. Section 2 discusses the robustness of multiple subpolar gyre (SPG) modes by presenting findings from several climate models. Section 3 continues this discussion summarizing work on the sensitivity of the SPG primarily in CLIM*BER*-3α. This is followed by figures supporting conclusions in the main text and a table referencing the marine sediment cores discussed in the main text in section 4.

---

[1] Corresponding author: andreas.born@bjerknes.uib.no

1 The climate model CLIM*BER*-3α and experimental design

CLIM*BER*-3α consists of the statistical-dynamical atmosphere model POTSDAM-2 (*Petoukhov et al.*, 2000) coupled to a global ocean general circulation model based on the Geophysical Fluid Dynamics Laboratory (GFDL) Modular Ocean Model (MOM-3) code and to the dynamic and thermodynamic sea ice module of *Fichefet and Maqueda* (1997). The oceanic horizontal resolution is $3.75° \times 3.75°$ with 24 unevenly spaced vertical layers. We apply a weak background vertical diffusivity of $0.2 \times 10^{-4} m^2 s^{-1}$. For a discussion on the model's sensitivity to this parameter refer to *Mignot et al.* (2006). The implemented second-order moment tracer advection scheme (*Prather*, 1986) minimizes numerical diffusion (*Hofmann and Maqueda*, 2006). The model makes use of a parametrization of boundary enhanced mixing depending both on near-bottom stratification and roughness of topography (*Ledwell et al.*, 2000), following *Hasumi and Suginohara* (1999). This leads locally to vertical diffusion coefficients of up to $10^{-4} m^2 s^{-1}$ for example over rough topography.

The atmosphere model has a coarse spatial resolution ($7.5°$ in latitude and $22.5°$ in longitude) and is based on the assumption of a universal vertical structure of temperature and humidity, which allows reducing the three-dimensional description to a set of two-dimensional prognostic equations. Description of atmospheric dynamics is based on a quasi-geostrophic approach and a parametrization of the zonally averaged meridional atmospheric circulation. Synoptic processes are parametrized as diffusion terms with a turbulent diffusivity computed from atmospheric stability and horizontal temperature gradients. Heat and freshwater fluxes between ocean and atmosphere are computed on the oceanic grid and applied without any flux adjustments. The wind stress is computed as the sum of the NCEP-NCAR reanalysis wind stress climatology (*Kalnay and coauthors*, 1996) and the wind stress anomaly calculated by the atmospheric model relative to the control run. CLIM*BER*-3α has been validated against data both for Holocene (*Montoya et al.*, 2005) and glacial boundary conditions (*Montoya and Levermann*, 2008).

Deep water formation takes place in two regions, north of the Greenland Scotland ridge and in the SPG center. Deep water masses are communicated by overflows

through the deepest passages of the ridge. This deep outflow from the Nordic Seas facilitates a surface inflow in our model. Although only crudely represented, the exchange shows the dynamical behavior expected from Holocene paleo data (*Solignac et al.*, 2004) and model studies (*Renssen et al.*, 2005).

2 Evidence for multiple subpolar gyre modes in other models

The positive feedbacks that give rise to the SPG bistability are based exclusively on large scale dynamics. Thus, they are likely to be found in most ocean models even though the existence of multiple stable SPG modes circulation might be masked by other processes. While there are good indications from proxy data that a transition between two SPG modes took place indeed and was not masked by such secondary processes, here we shortly present some fundamental considerations regarding the existence of positive SPG feedbacks and discuss indications for these feedbacks in a number of different ocean models.

Convection in the SPG center is intimately linked to its strength (*Eden and Willebrand*, 2001; *Häkkinen and Rhines*, 2004; *Treguier et al.*, 2005; *Born et al.*, 2010a), because it increases density in the gyre's center around which water circulates baroclinically (*Born et al.*, 2009). Thus the bistability of the SPG circulation can also be understood in the framework of convection, with stronger convection entailing a stronger gyre. In addition, a stronger SPG advects more saline water into the western North Atlantic facilitating convection, a positive feedback that destabilizes the system (*Levermann and Born*, 2007).

Different modes of Labrador Sea deep convection are found in many ocean models. In HadCM3, *Kleinen et al.* (2009) discuss a 70 % weakening of the SPG coeval with a reduction of Labrador Sea convection in response to continuous freshwater forcing of the North Atlantic. Experiments with anomalous heat transports over Labrador Sea by *Wu and Wood* (2008) exhibit an abrupt strengthening of the SPG for higher heat loss and convection. A weaker SPG circulation in response to weaker convection in its center has also been confirmed for the Institut Pierre Simon Laplace Coupled

3

Model 4 (IPSL CM4) (*Born et al.*, 2010a). The positive feedback related to a weaker salt transport by the SPG was also quantified in this study.

In addition to *Levermann and Born* (2007), some further studies directly report on spontaneous transitions between active and inactive Labrador Sea convection modes. These suggest the presence of destabilizing positive feedbacks. *Jongma et al.* (2007) discuss a bistability of convection and overturning circulation. Their model (ECBilt-Clio) alternates between two meta-stable states with active and inactive convection. Along with an externally applied constant freshwater perturbation over Labrador Sea, the residence time in the inactive convection state gradually increases. *LeGrande et al.* (2006) and *LeGrande and Schmidt* (2008) also find a spontaneous transition to active Labrador Sea convection in their preindustrial control run with the Goddard Institute for Space Studies ModelE-R atmosphere ocean general circulation model. Two states of SPG circulation have also been observed in the Bergen Climate Model, an AOGCM (H. Drange, personal communication, 2009).

While models over a wide range of complexity suggest the existence of multiple SPG modes, earlier model simulations of the 8.2k event did not report persistent changes in the SPG circulation. Without the coeval intensification of deepwater formation south of the Greenland Scotland ridge, these models usually report a strong reduction of the Atlantic Meridional Overturning Circulation (AMOC), an apparent contradiction of our results. This is possibly due to the direct application of the meltwater pulse on the Labrador Sea convection region. As pointed out above, convection in the gyre's center has strong control on its strength, which will be discussed in more detail in the following section. *Bauer et al.* (2004) employ a zonally averaged, two-dimensional, ocean model. Hence, the freshwater anomaly is distributed over the entire basin width and inevitably affects convection south of the Greenland Scotland ridge directly. Moreover, gyre dynamics cannot be adequately included in zonally averaged models. *LeGrande et al.* (2006) and *LeGrande and Schmidt* (2008) simulate the 8.2k event in a three-dimensional ocean model using two different initial states. One result is that the state more realistic for the early Holocene, with weak Labrador Sea convection, simulates a significantly weaker AMOC reduction (30 %) than the strong initial state (50 %). This supports our findings that it is important not to apply the meltwater pulse directly on the convection region. *Wiersma et al.*

(2006) also report a weaker AMOC reduction when applying the meltwater pulse on a weak Labrador Sea convection state. However, in this study the meltwater pulse is applied in the center of the Labrador Sea and directly on the convection region, which is still active in the weak state. This forcing scenario favors a strong AMOC response but disagrees with paleo data (*Hillaire-Marcel et al.*, 2007; *Keigwin et al.*, 2005) and a high resolution model study (*Winsor et al.*, 2006). Another consequence of applying the meltwater pulse directly onto the Labrador Sea convection region is that it removes a significant fraction of the meltwater pulse from the surface. Hence, a smaller fraction is advected into the Nordic Seas. This, however, is crucial to initiate the mechanism amplifying the SPG as has been shown in the main text.

3   Model sensitivity of the subpolar gyre circulation to changes in external forcing

The strength of the SPG depends at least partially on the density gradient between its center and rim. The water column in the center is relatively denser, causing a depression in sea surface height around which water circulates cyclonically in geostrophic balance. Increasing this density gradient results in a deeper depression and a stronger gyre. This understanding differentiates two classes of mechanisms controlling the SPG strength, by modifying the density of the water column in its center or the rim (Fig. S1).

3.1   Sensitivity to the representation of Greenland Scotland ridge overflow and anomalous freshwater forcing

Density at the northern rim of the SPG is partially controlled by dense waters overflowing the Greenland Scotland ridge. Because the representation of these small scale currents is essential for the formation of North Atlantic Deep Water but problematic in ocean general circulation models, it is often enhanced by means of numerical techniques. A study of two different approaches, namely artificial deepending of the ridge and a hydraulic overflow parametrization, found that both simulate the large
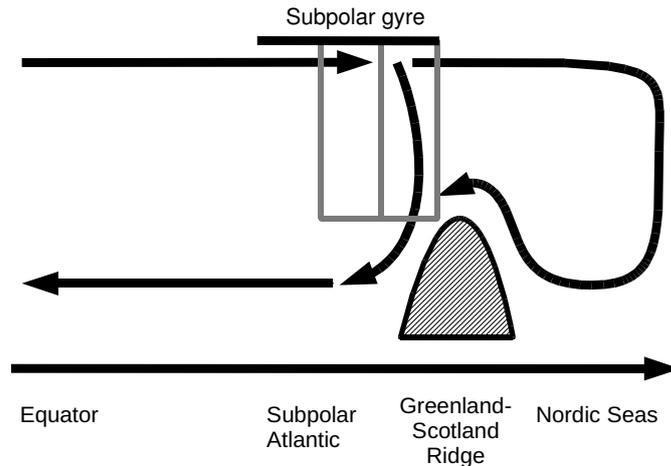
Figure S1: Schematic of the Atlantic Meridional Overturning Circulation (AMOC) and the subpolar gyre. Grey boxes show the center and exterior regions of the gyre referred to in the main text. Density changes in the center region are the result of positive feedbacks inherent to the subpolar gyre. The density on its rim is determined by two water masses mixing at intermediate depth, the denser one reaching the mixing region after sinking in the Nordic Seas and overflowing the Greenland-Scotland ridge and a second produced by sinking south of the ridge.

scale deep ocean circulation similarly well. However, the density of the resulting water mass south of the Greenland Scotland ridge, thus at the SPG rim, is lower in one case resulting in a significantly stronger SPG (*Born et al.*, 2009).

Besides continuous changes in the overflow transport, we also investigated the sensitivity of the SPG to a transient reduction in overflow strength in response to anomalous freshwater flux into the Nordic Seas (*Levermann and Born*, 2007). Two main conclusions can be drawn from this study. First, the increase in SPG strength persists even after the freshwater pulse. This illustrates the relative importance of reduced overflows and density in the SPG rim on one side to positive feedbacks of the SPG that increase the density in the gyre's center on the other, while both mechanisms strengthen the circulation. Once the SPG reaches a critical strength due to the overflows reduction, the SPG feedbacks increase the density in the SPG center and stabilize the strong circulation mode. Secondly, a freshwater pulse of 0.05 Sv over 25 years is sufficient to trigger a notable increase in SPG strength (Fig. S2). This is about a fourth of the lake Agassiz drainage volume and a good

approximation to the fraction of the drainage that is advected into the Nordic Seas over a similar period of time ($\sim$ 30 years, Fig. 4 in the main text). This earlier sensitivity study strongly supports the simulation presented here for the 8.2k event.

The dilution of the lake drainage before reaching the main impact region, the Nordic Seas, the multi-decadal delay due to advection and the fact that a fraction of the original freshwater volume is enough to trigger the transition helps to assess the importance of a possible multipulse event of two smaller volume discharges as proposed from observations (*Ellison et al.*, 2006).
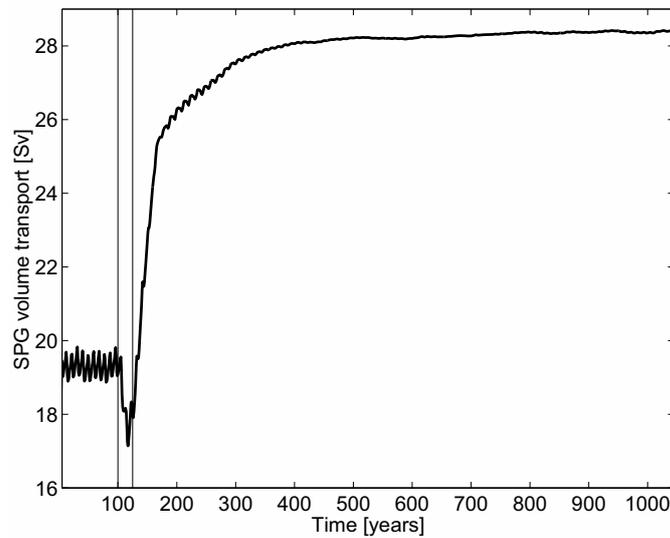

Figure S2: Temporal evolution of the SPG strength in response to freshwater forcing in the Nordic Seas. The vertical lines indicates the forcing period (25 years).

3.2   Sensitivity to wind stress

The transition of the SPG is robust to fixed surface wind stress (Fig. S3). In our model, the applied surface wind stress is generally based on anomalies from the atmospheric model added to climatological averages. We repeated the experiment presented in *Levermann and Born* (2007) with surface wind stress prescribed to climatology in order to test the sensitivity of the SPG transition to this technique.

In addition, the sensitivity to scalar multiples of the climatological wind stress
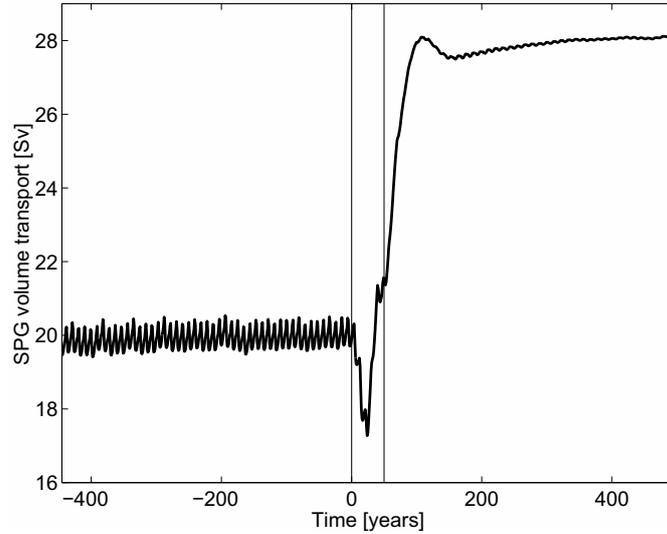
7

Figure S3: Temporal evolution of the SPG strength for an experiment with winds stress prescribed to present day climatology.

ranging over $\alpha \in [0.25, 2]$ has been investigated in preindustrial and Last Glacial Maximum (LGM) climate (*Montoya et al.*, 2010). The SPG strength is found to be considerably stronger in preindustrial than in LGM experiments, showing a qualitatively different sensitivity to surface wind stress. Under preindustrial boundary conditions, it decreases with increasing wind stress. Under LGM boundary conditions, it generally increases linearly with wind stress extrapolating to zero for zero wind stress. However, beyond a certain threshold for the wind stress the SPG sensitivity is reversed in the LGM and decreases with wind stress as well. This threshold is associated with the initiation of deep water formation in the Nordic Seas and the accompanying intensification of the Greenland Scotland ridge overflows.

Hence, even for changes in surface wind stress, the primary means of communicating this perturbation to the SPG is the overflow transport. This result from a fundamentally different set of experiments underlines the pivotal role of deep ocean baroclinicity for the sensitivity of the SPG and supports the findings of the present study.

8

3.3 Sensitivity to vertical mixing

The bistability of the SPG is robust to changes in vertical diffusivity. Global background diffusivity in our model is $\kappa = 0.2 \times 10^{-4} m^2 s^{-1}$. However, experiments with $\kappa = 0.5 \times 10^{-4} m^2 s^{-1}$ also show two stable SPG modes and with even larger contrast in strength (Fig. S4).
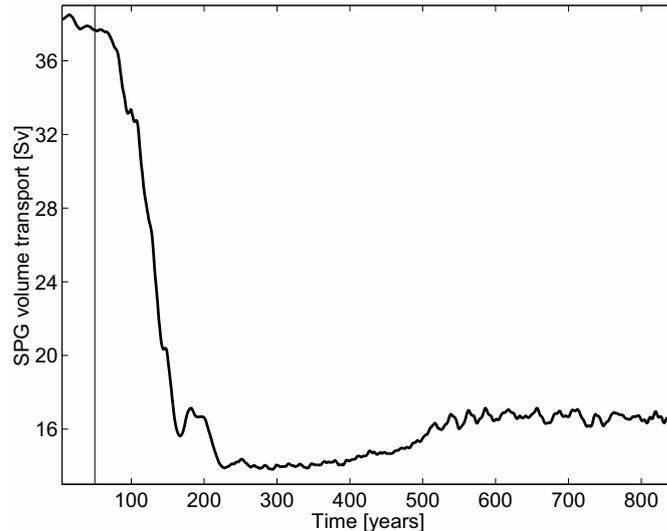

Figure S4: Temporal evolution of the SPG strength in a model version with higher vertical diffusivity. Starting from the strong circulation mode, a negative freshwater pulse of 0.1 Sv is applied over the first 50 years.

Multiple SPG equilibria are also found in a more fundamentally altered model set up. *Marzeion et al.* (2010) implemented a stratification-dependent mixing scheme and forced the model with an 1%-per-year increase scenario of atmospheric CO_2. Warming and enhanced freshwater influx reduce the surface density of the North Atlantic as the CO_2 concentration increases. This results in stronger stratification, thus weaker vertical mixing and a density increase in subsurface water masses that feed the Greenland Scotland ridge. If the sensitivity of the mixing to stratification is raised above a certain critical level, the weakening of the SPG is enhanced by the positive feedbacks described by *Levermann and Born* (2007).

3.4   Sensitivity to orbital parameters changes

The simulation of lake Agassiz drainage with preindustrial boundary conditions, i.e. with lower northern hemisphere summer insolation levels, gives a similar result (Fig. S5). This demonstrates the strength and robustness of the feedbacks involved.

However, with an even bigger change in orbital geometry one or the other circulation mode is preferred in CLIM*BER*-3α and IPSL CM4 (*Born et al.*, 2010a,b). A decrease in northern hemisphere summer insolation between 126,000 and 115,000 years before present is most pronounced in high northern latitudes. It thus favors Arctic sea ice growth causing an increase in sea ice export and a freshening south of Greenland. As a consequence, convection in the center of the SPG shuts down, density in the SPG center decreases and the gyre weakens. The analysis of the underlying dynamics confirm that the reorganization of the subpolar surface circulation is due to the same mechanism in both models indeed. However, changes in Arctic sea ice are much smaller for the simulated freshwater flood in this study and probably do not play a role for the stabilization of the circulation.
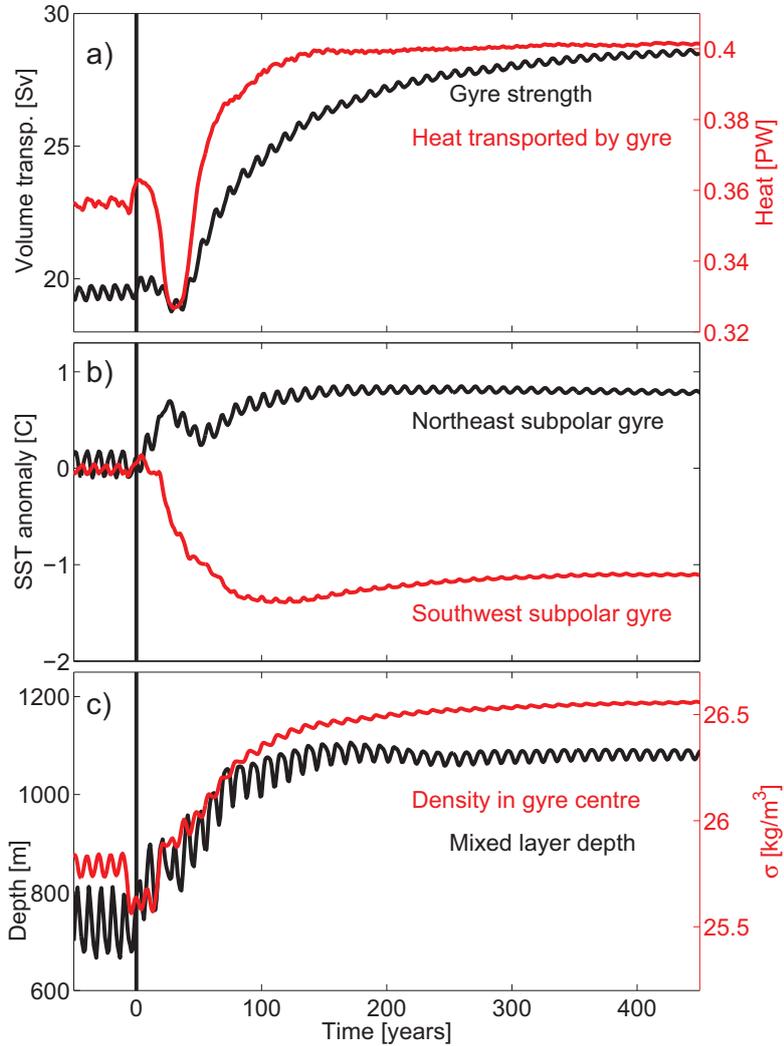
Figure S5: Simulation of the lake drainage in preindustrial climate, similar to figure 3 of the main text. The vertical line indicates the timing of the freshwater perturbation, data is filtered with a 25-year running mean. **a)** Volume and heat transport of the SPG; **b)** sea surface temperature in the north-eastern (black) and south-western (red) subpolar region; **c)** maximum winter mixed layer depth in the center of the SPG and surface density in the center of the SPG (see Fig. S7). The transition of the SPG and the underlying feedbacks are robust to a change in orbital geometry.

11

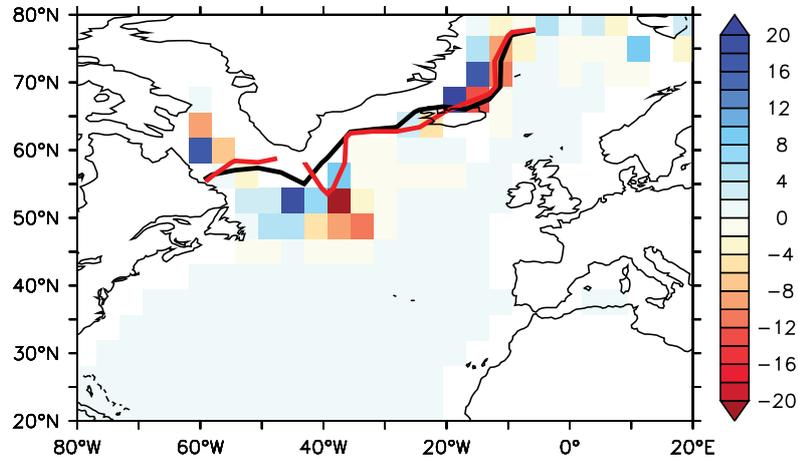# 4 Supplemental figures and list of sediment cores

Figure S6: Colors: percental change in wind stress curl 'after' minus 'before' melt-water pulse; Contours: 15% sea ice concentration January to March average after (black) and before (red) transition. Wind stress curl changes are small, below 20% compared to the 47% strengthening of the SPG, and do not show a consistent pattern. Potential upwind changes in elevation, albedo or heat capacity due to the lake drainage are neglected in the model. Thus, the shown wind stress curl anomalies are likely due to local changes in sea ice as suggested also by the irregular pattern.
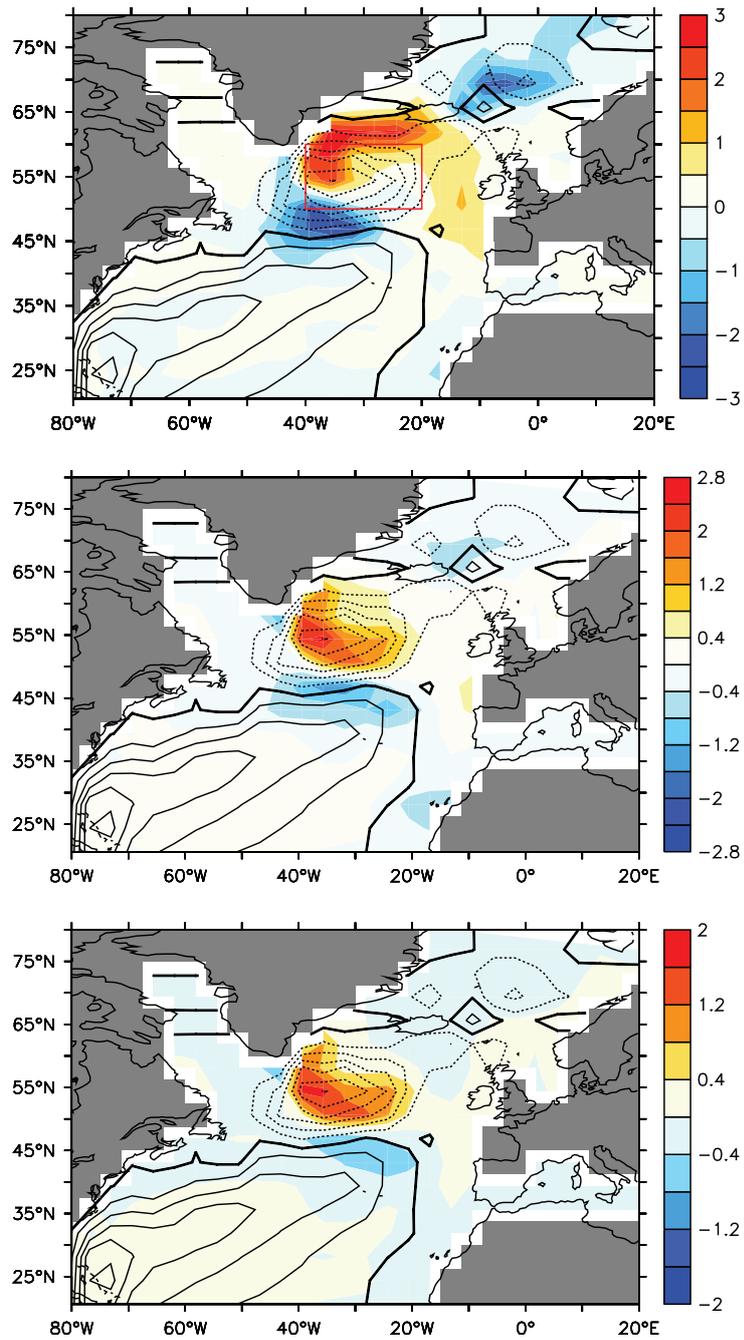
Figure S7: Difference 'after' minus 'before' meltwater pulse, averaged annually and over the upper 75m: temperature (in °C, upper), salinity (in psu, middle), and density (in kg m^{-3}, lower). Steamlines indicate the location of the subpolar gyre after the transition. The region used for averages in figures 3 of the main text and S8 is shown in red.
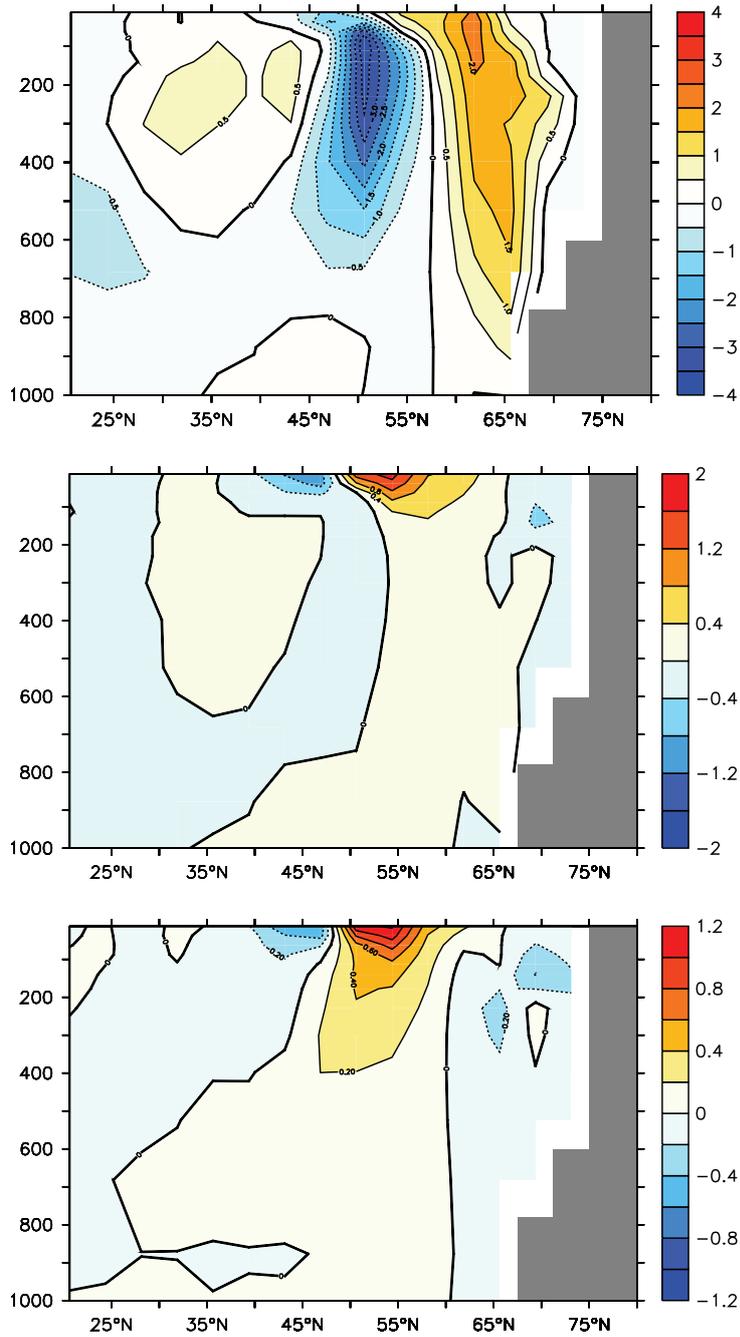
Figure S8: Difference 'after' minus 'before' meltwater pulse, averaged annually and between 40°W and 20°W: temperature (in °C, upper), salinity (in psu, middle), and density (in kg m^{-3}, lower). The largest difference in salinity is seen on the surface due to changes in the advection. In contrast, temperature changes change primarily in subsurface waters because of stronger isopycnal mixing and convection.
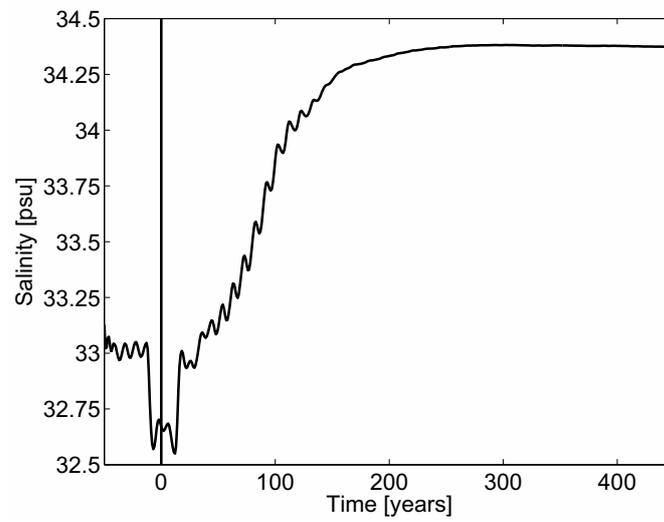
Figure S9: Temporal evolution of annual average sea surface salinity in the center of the subpolar gyre, averaged between 50°N and 60°N and 40°W and 20°W (red rectangle in fig. S7) and filtered with a 25-year running mean. The vertical line indicates the simulated lake Agassiz drainage.

15

Table S1: List of marine sediment cores used in this study. Magnitude (ΔSST), start of the SPG transition and proxy method are shown where applicable.

Abbreviation in Fig. 1	Full name	ΔSST (°C)	Start (yr BP)	Method	References
HU13	HU90–013–013P	-3	8,200	dinocyst assemblages	Hillaire-Marcel et al. (2001) Solignac et al. (2004) de Vernal and Hillaire-Marcel (2006)
HU21	HU84–030–021TWC&P	-5	8,500	dinocyst assemblages	de Vernal and Hillaire-Marcel (2006) Hillaire-Marcel et al. (2001)
HU94	HU91–045–094P	-5	7,800	dinocyst assemblages	Solignac et al. (2004) de Vernal and Hillaire-Marcel (2006)
OCE326 –GGC26	OCE326–GGC26	-3	8,000	alkenones	Keigwin et al. (2005) Sachs (2007)
LO09-14	LO09-14 LBC/GGC/GC	+2.5	8,000	diatoms	Andersen et al. (2004)
ODP984	ODP Site 984	+1.5	8,000	Mg/Ca	Came et al. (2007)
MD2251	MD99–2251			sortable silt	Ellison et al. (2006)
MD2665	MD03–2665			δ^{13}C & grain size	Kleiven et al. (2008)
NEAP4k	NEAP4k			sortable silt	Hall et al. (2004)

16

References

Andersen, C., N. Koc, and M. Moros (2004), A highly unstable Holocene climate in the subpolar North Atlantic: evidence from diatoms, *Quaternary Science Reviews*, *23*, 2155–2166.

Bauer, E., A. Ganopolski, and M. Montoya (2004), Simulation of the cold climate event 8200 years ago by meltwater outburst from Lake Agassiz, *Paleoceanography*, *19*, PA3014.

Born, A., A. Levermann, and J. Mignot (2009), Sensitivity of the Atlantic ocean circulation to a hydraulic overflow parameterisation in a coarse resolution model: Response of the subpolar gyre, *Ocean Modelling*, *27 (3-4)*, 130–142.

Born, A., K. H. Nisancioglu, and P. Braconnot (2010a), Sea ice induced changes in ocean circulation during the Eemian, *Climate Dynamics*, *online*, doi: 10.1007/s00382-009-0709-2.

Born, A., K. H. Nisancioglu, B. Risebrobakken, and A. Levermann (2010b), Late Eemian warming in the Nordic Seas as seen in proxy data and climate models, *Paleoceanography*, *in revision*.

Came, R. E., D. W. Oppo, and J. F. McManus (2007), Amplitude and timing of temperature and salinity variability in the subpolar North Atlantic over the past 10 k.y., *Geology*, *35*, 315–318.

de Vernal, A., and C. Hillaire-Marcel (2006), Provincialism in trends and high frequency changes in the northwest North Atlantic during the Holocene, *Global and Planetary Change*, *54*, 263–290.

Eden, C., and J. Willebrand (2001), Mechanism of Interannual to Decadal Variability of the North Atlantic Circulation, *Journal of Climate*, *14*, 2266–2280.

Ellison, C. R. W., M. R. Chapman, and I. R. Hall (2006), Surface and Deep Ocean Interactions During the Cold Climate Event 8200 Years Ago, *Science*, *312*, 1929–1932.

Fichefet, T., and M. A. M. Maqueda (1997), Sensitivity of a global sea ice model to the treatment of ice thermodynamics and dynamics, *Journal of Geophysical Research*, *102*, 12,609.

Häkkinen, S., and P. B. Rhines (2004), Decline of subpolar North Atlantic circulation during the 1990s, *Science*, *304*, 555–559.

Hall, I. R., G. Bianchi, and J. R. Evans (2004), Centennial to millenial scale Holocene climate-deep water linkage in the North Atlantic, *Quaternary Science Reviews*, *23*, 1529–1536.

Hasumi, H., and N. Suginohara (1999), Effects of locally enhanced vertical diffusivity over rough bathymetry on the world ocean circulation, *Journal of Geophysical Research*, *104*, 23,364–23,374.

Hillaire-Marcel, C., A. de Vernal, A. Bilodeau, and A. J. Weaver (2001), Absence of deep-water formation in the Labrador Sea during the last interglacial period, *Nature*, *410*, 1073–1077.

Hillaire-Marcel, C., A. de Vernal, and D. J. W. Piper (2007), Lake Agassiz Final drainage event in the northwest North Atlantic, *Geophysical Research Letters*, *34*, L15,601.

Hofmann, M., and M. A. M. Maqueda (2006), Performance of a second-order moments advection scheme in an Ocean General Circulation Model, *Journal of Geophysical Research*, *111*, C05,006.

Jongma, J., M. Prange, H. Renssen, and M. Schulz (2007), Amplification of Holocene multicentennial climate forcing by mode transitions in North Atlantic overturning circulation, *Geophysical Research Letters*, *34*, L15,706.

Kalnay, E., and coauthors (1996), The NCEP/NCAR 40-year reanalysis project, *Bull. Amer. Meteor. Soc.*, *77*, 437–471.

Keigwin, L. D., J. P. Sachs, Y. Rosenthal, and E. A. Boyle (2005), The 8200 year B.P. event in the slope water system, western subpolar North Atlantic, *Paleoceanography*, *20*, PA2003.

18

Kleinen, T., T. J. Osborn, and K. R. Briffa (2009), Sensitivity of climate response to variations in freshwater hosing location, *Ocean Dynamics*, *59(3)*, 509–521, doi:10.1007/s10236-009-0189-2.

Kleiven, H. F., C. Kissel, C. Laj, U. S. Ninnemann, T. O. Richter, and E. Cortijo (2008), Reduced North Atlantic Deep Water Coeval with the Glacial Lake Agassiz Fresh Water Outburst., *Science*, *319*, 60–64.

Ledwell, J. R., E. T. Montgomery, K. L. Polzin, L. C. S. Laurent, R. W. Schmitt, and J. M. Toole (2000), Evidence for enhanced mixing over rough topography in the abyssal ocean, *Nature*, *403*, 179–182.

LeGrande, A. N., and G. A. Schmidt (2008), Ensemble, water isotope-enabled, coupled general circulation modeling insights into the 8.2 ka event, *Paleoceanography*, *23*, PA3207.

LeGrande, A. N., G. A. Schmidt, D. T. Shindell, C. V. Field, R. L. Miller, D. M. Koch, G. Faluvegi, and G. Hoffmann (2006), Consistent simulations of multiple proxy responses to an abrupt climate change event, *Proceedings of the National Academy of Sciences (US)*, *103*, 837–842.

Levermann, A., and A. Born (2007), Bistability of the Atlantic subpolar gyre in a coarse-resolution model, *Geophysical Research Letters*, *34*, L24,605.

Marzeion, B., A. Levermann, and J. Mignot (2010), Sensitivity of North Atlantic subpolar gyre and overturning to stratification-dependent mixing: response to global warming, *Climate Dynamics*, *online*, doi:10.1007/s00382-008-0521-4.

Mignot, J., A. Levermann, and A. Griesel (2006), A decomposition of the Atlantic meridional overturning circulation into physical components using its sensitivity to vertical diffusivity., *Journal of Physical Oceanography*, *36*, 636–650.

Montoya, M., and A. Levermann (2008), Surface wind stress threshold for glacial Atlantic overturning, *Geophysical Research Letters*, *35*, L03,608.

Montoya, M., A. Griesel, A. Levermann, J. Mignot, M. Hofmann, A. Ganopolski, and S. Rahmstorf (2005), The Earth System Model of Intermediate Complexity

CLIM*BER*-3α. Part I: description and performance for present-day conditions, *Climate Dynamics*, *25*, 237–263.

Montoya, M., A. Born, and A. Levermann (2010), Reversed North Atlantic gyre dynamics in glacial climate, *Climate Dynamics*, *online*, doi:10.1007/s00382-009-0729-y.

Petoukhov, V., A. Ganopolski, V. Brovkin, M. Claussen, A. Eliseev, C. Kubatzki, and S. Rahmstorf (2000), CLIM*BER*-2: a climate system model of intermediate complexity. Part I: model description and performance for present climate, *Climate Dynamics*, *16*, 1.

Prather, M. J. (1986), Numerical advection by conservation of second-order moments, *Journal of Geophysical Research*, *91*, 6671–6681.

Renssen, H., H. Goosse, and T. Fichefet (2005), Contrasting trends in North Atlantic deep-water formation in the Labrador Sea and Nordic Seas during the Holocene, *Geophysical Research Letters*, *32*, L08,711.

Sachs, J. P. (2007), Cooling of Northwest Atlantic slope waters during the Holocene, *Geophysical Research Letters*, *34*, L03,609.

Solignac, S., A. de Vernal, and C. Hillaire-Marcel (2004), Holocene sea-surface conditions in the North Atlantic–contrasted trends and regimes in the western and eastern sectors (Labrador Sea vs. Iceland Basin), *Quaternary Science Reviews*, *23*, 319–334.

Treguier, A. M., S. Theetten, E. P. Chassignet, T. Penduff, R. Smith, L. Talley, J. O. Beismann, and C. Böning (2005), The North Atlantic Subpolar Gyre in Four High-Resolution Models, *Journal of Physical Oceanography*, *35*, 757–774.

Wiersma, A. P., H. Renssen, H. Goosse, and T. Fichefet (2006), Evaluation of different freshwater forcing scenarios for the 8.2 ka BP event in a coupled climate model, *Climate Dynamics*, *27*, 831–849.

Winsor, P., L. Keigwin, S. J. Lentz, and D. C. Chapman (2006), The pathways and impact of fresh water discharge through Hudson Strait 8200 years ago, *Geophysical Research Abstracts*, *8*, 11,007.

Wu, P., and R. A. Wood (2008), Convection induced long term freshening of the subpolar North Atlantic Ocean, *Climate Dynamics*, *31*, 941–956.